Introduction to Nuclear and Particle Physics

α decay

Helga Dénes 2022 Yachay Tech

hdenes@yachaytech.edu.ec

Decays

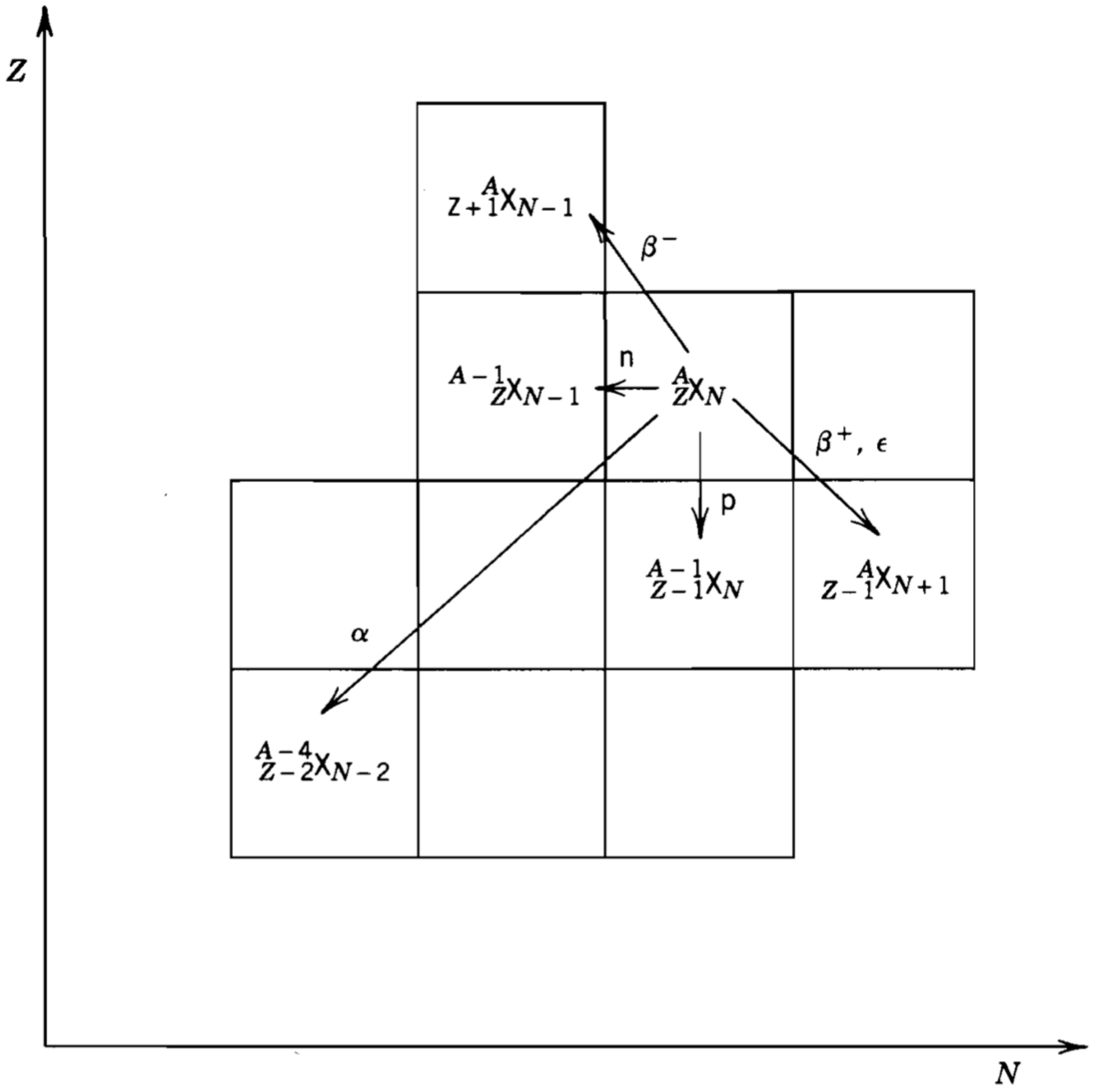

Figure 6.9 The initial nucleus $^{A}_{Z}X_{N}$ can reach different final nuclei through a variety of possible decay processes.

Q vs. half-life

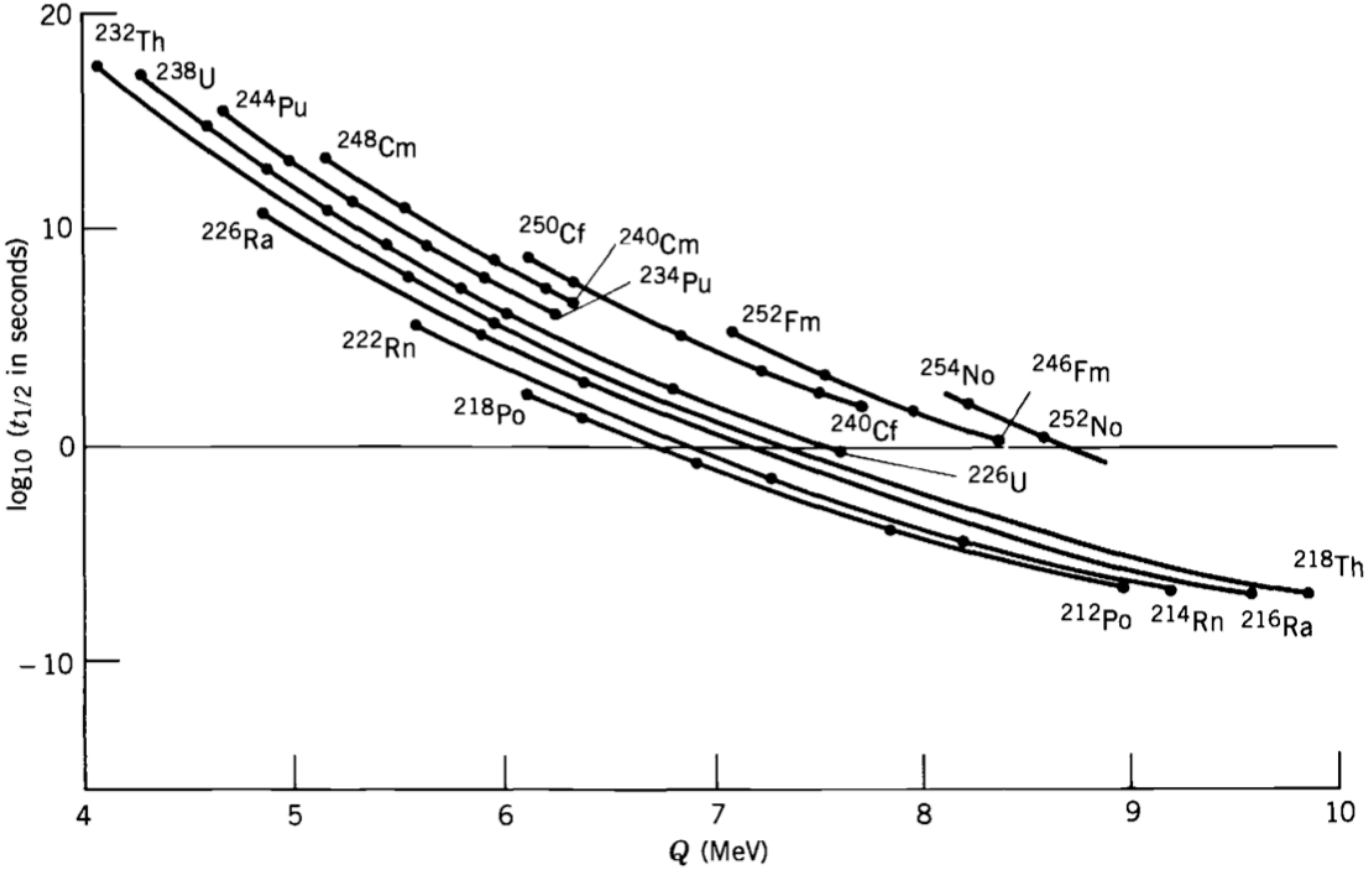

Figure 8.1 The inverse relationship between α-decay half-life and decay energy, called the Geiger-Nuttall rule. Only even-Z, even-N nuclei are shown. The solid lines connect the data points.

A vs. Q

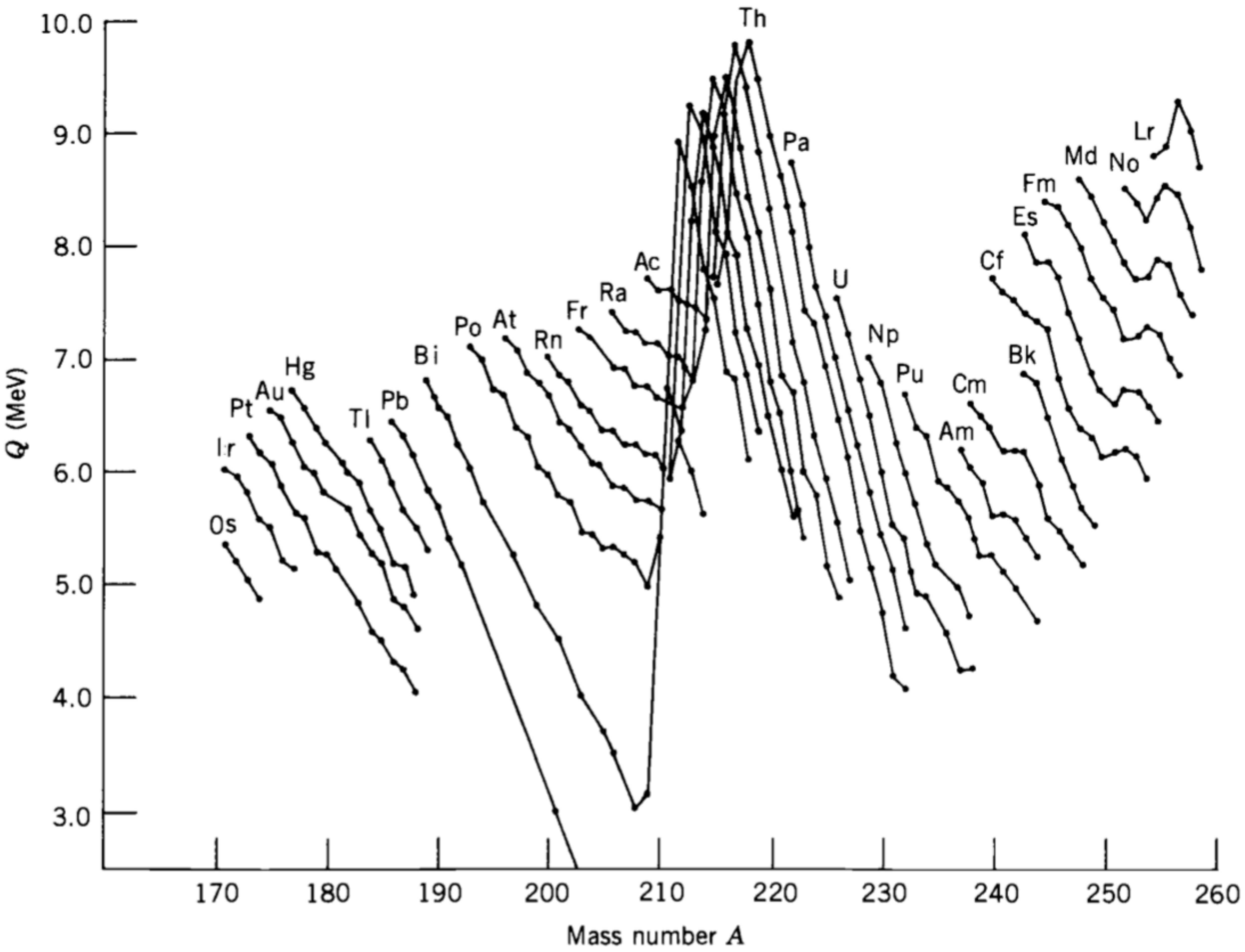

Figure 8.2 Energy released in α decay for various isotopic sequences of heavy nuclei. In contrast to Figure 8.1, both odd-A and even-A isotopes are shown, and a small amount of odd-even staggering can be seen. The effects of the shell closures at $N = 126$ (large dip in data) and $Z = 82$ (larger than average spacing between Po, Bi, and Pb sequences) are apparent.

α decay

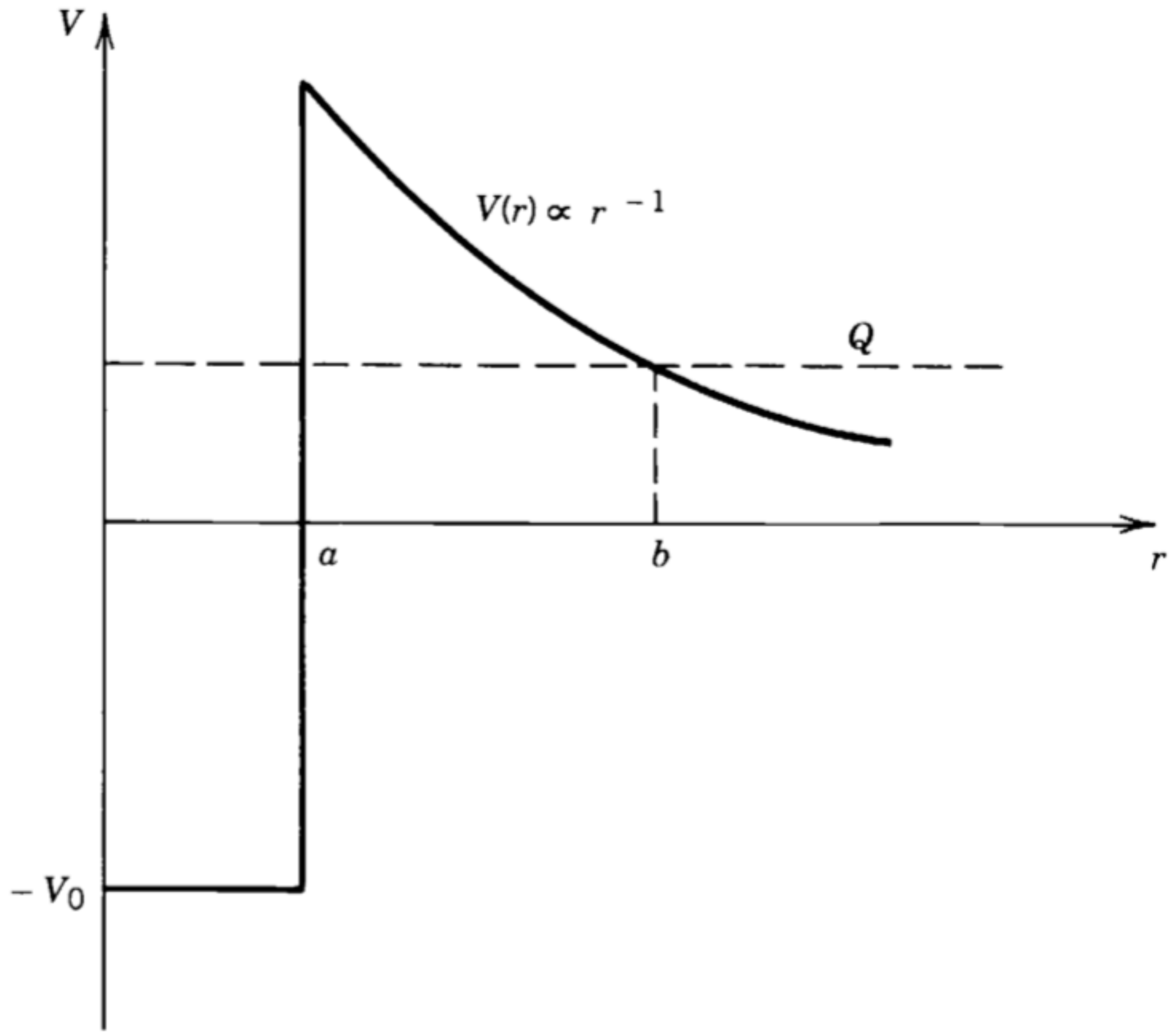

Figure 8.3 Relative potential energy of α-particle, daughter-nucleus system as a function of their separation. Inside the nuclear surface at $r = a$, the potential is represented as a square well; beyond the surface, only the Coulomb repulsion operates. The α particle tunnels through the Coulomb barrier from a to b.

α decay

Table 8.2 Calculated α-Decay Half-lives for Th Isotopes

A	Q (MeV)	$t_{1/2}$ (s)	
		Measured	Calculated
220	8.95	10^{-5}	3.3×10^{-7}
222	8.13	2.8×10^{-3}	6.3×10^{-5}
224	7.31	1.04	3.3×10^{-2}
226	6.45	1854	6.0×10^{1}
228	5.52	6.0×10^{7}	2.4×10^{6}
230	4.77	2.5×10^{12}	1.0×10^{11}
232	4.08	4.4×10^{17}	2.6×10^{16}

α decay

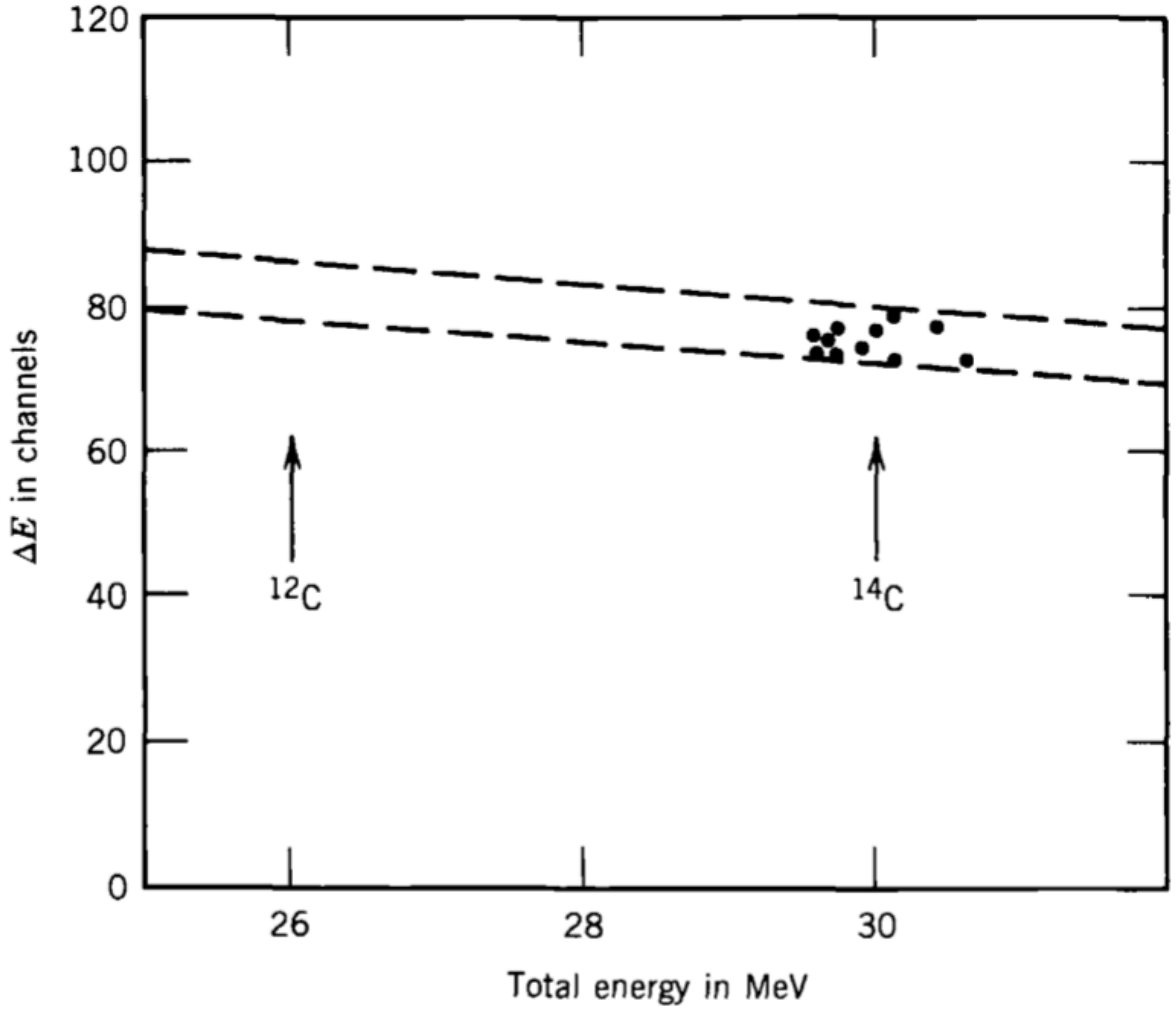

Figure 8.4 A portion of the tail of the $\Delta E \cdot T$ hyperbola showing the observed ^{14}C events from the decay of ^{223}Ra. The dashed lines show the limits expected for carbon. The 11 ^{14}C events result from 6 months of counting. From H. J. Rose and G. A. Jones, *Nature* **307**, 245 (1984). Reprinted by permission, copyright © Macmillan Journals Limited.

α decay

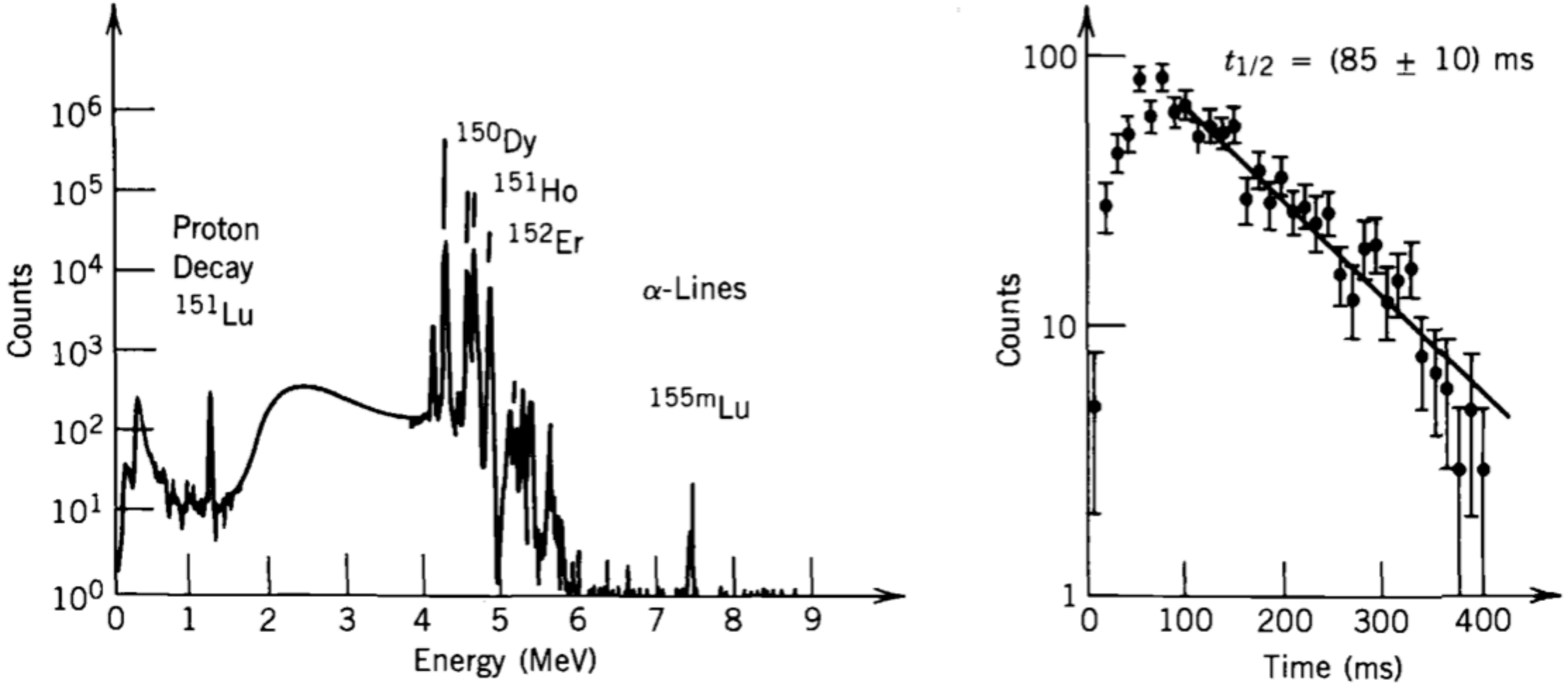

Figure 8.5 (Left) Charged-particle spectrum emitted in the radioactive decays of products of the reaction ^{96}Ru + ^{58}Ni. The peaks above 4 MeV represent α decays; the 1.2-MeV peak is from proton emission. (Right) The decay with time of the proton peak gives a half-life of 85 ms. From S. Hofmann et al., *Z. Phys. A* **305**, 111 (1982).

α decay

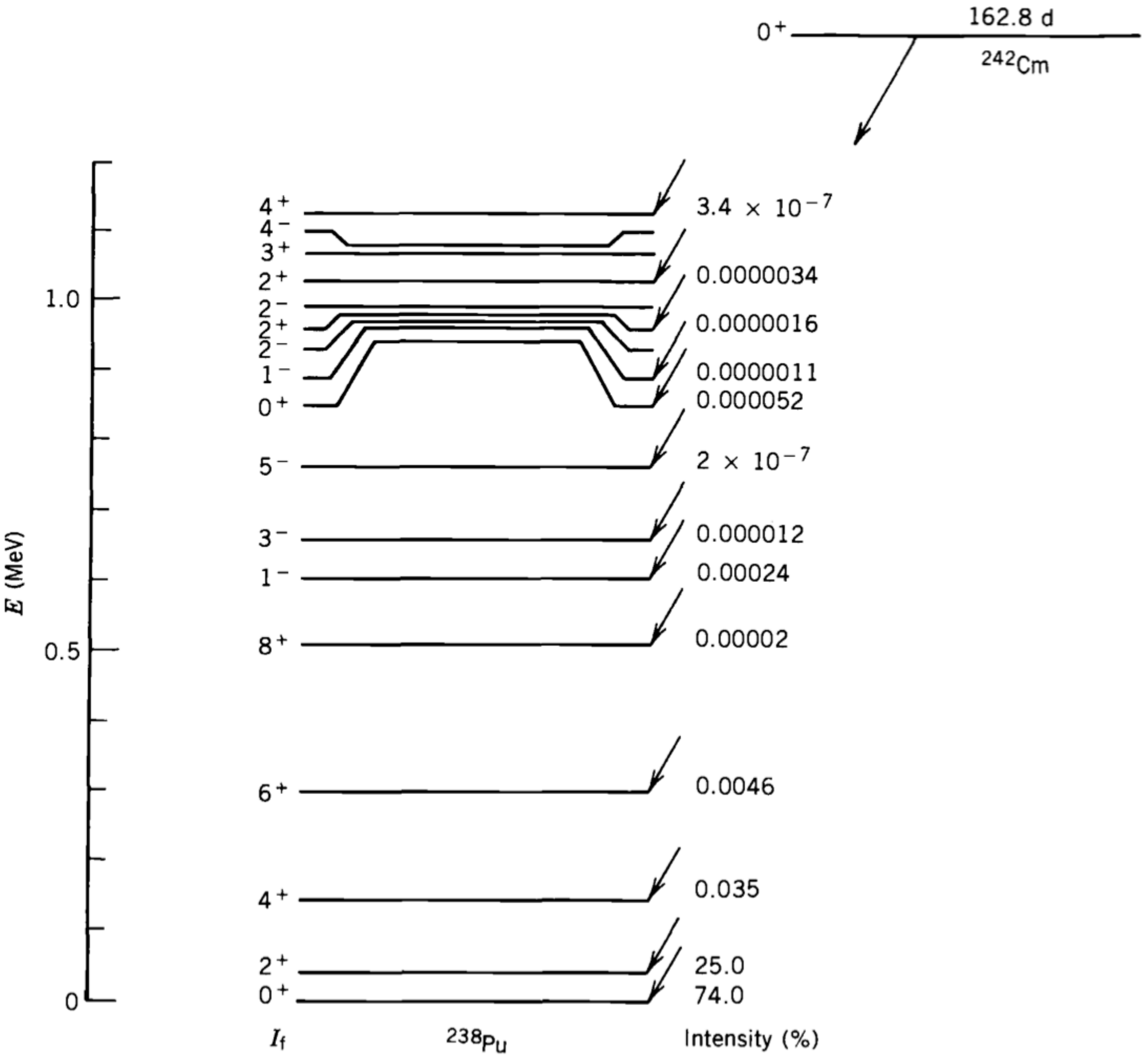

Figure 8.7 α decay of ^{242}Cm to different excited states of ^{238}Pu. The intensity of each α-decay branch is given to the right of the level.

α decay

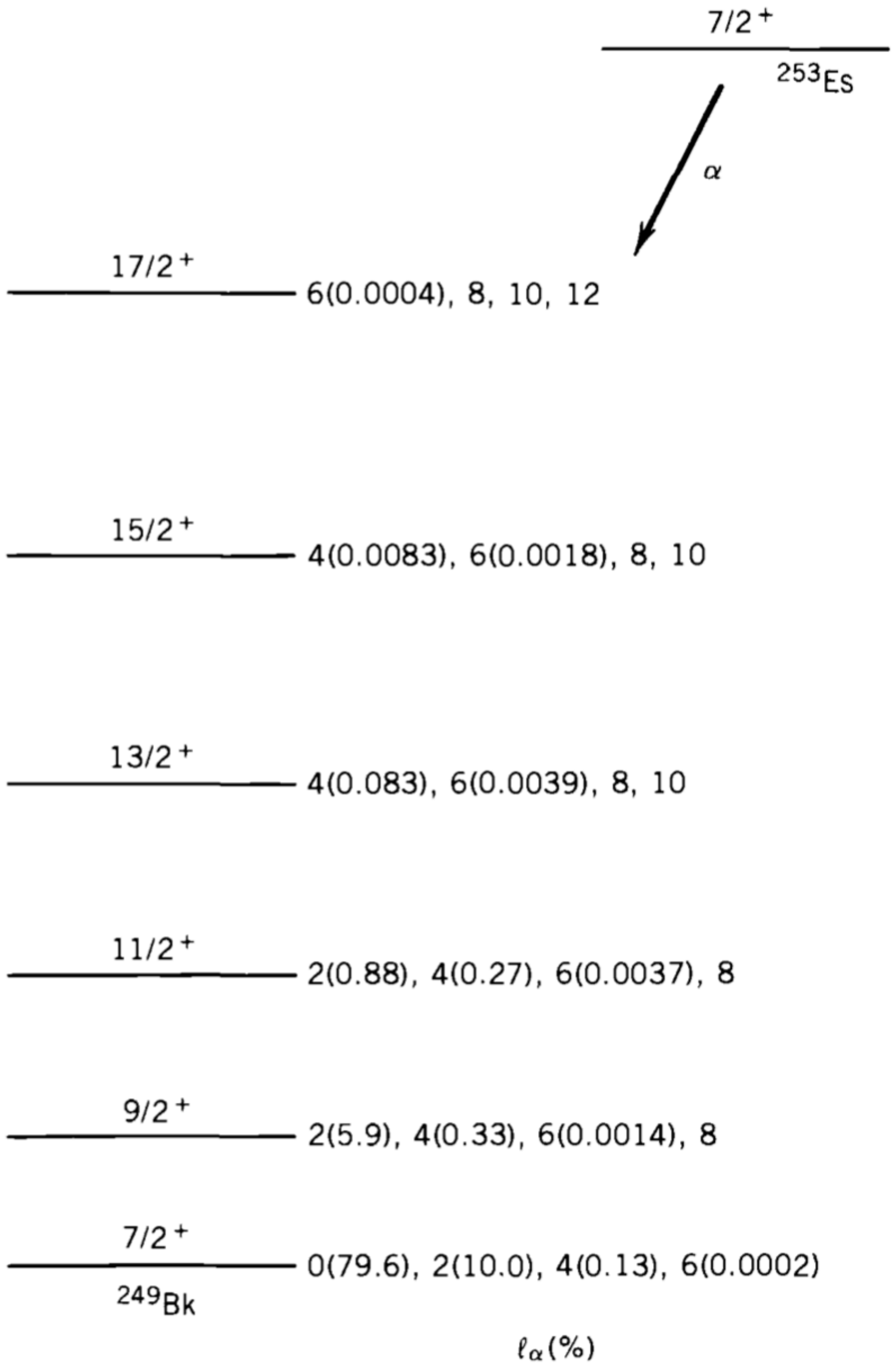

Figure 8.8 Intensities of various α-decay angular momentum components in the decay of ^{253}Es. For $\ell_\alpha = 8$ and higher, the intensities are not known but are presumably negligibly small. From the results of a study of spin-aligned α decays by A. J. Soinski et al., *Phys. Rev. C* **2**, 2379 (1970).

α decay

Lower barrier

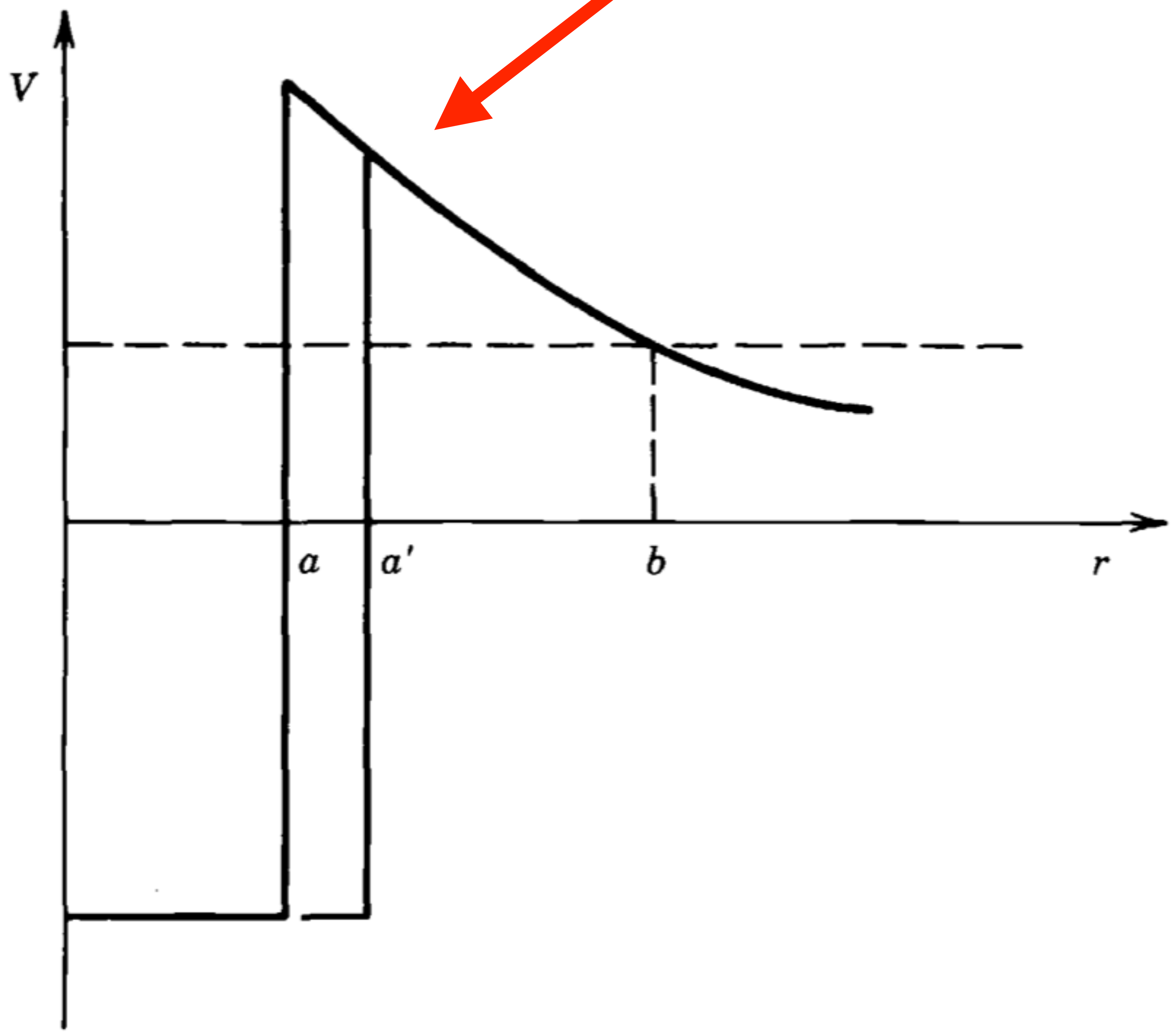

Figure 8.9 In a deformed nucleus, α particles escaping from the poles enter the Coulomb barrier at the larger separation a', and must therefore penetrate a lower, thinner barrier. It is therefore more probable to observe emission from the poles than from the equator.

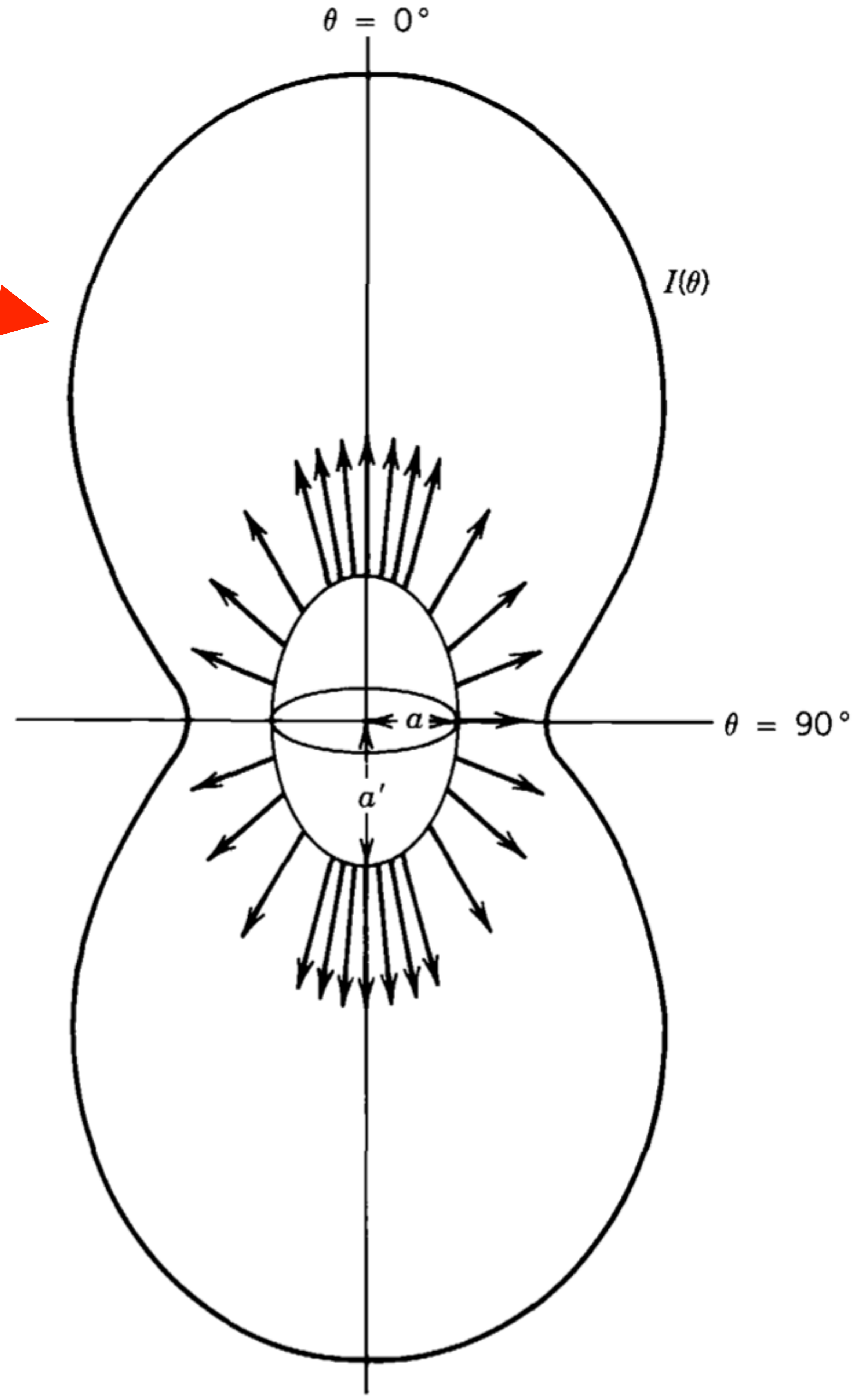

Figure 8.10 Intensity distribution of α particles emitted from the deformed nucleus at the center of the figure. The polar plot of intensity shows a pronounced angular distribution effect.

α decay

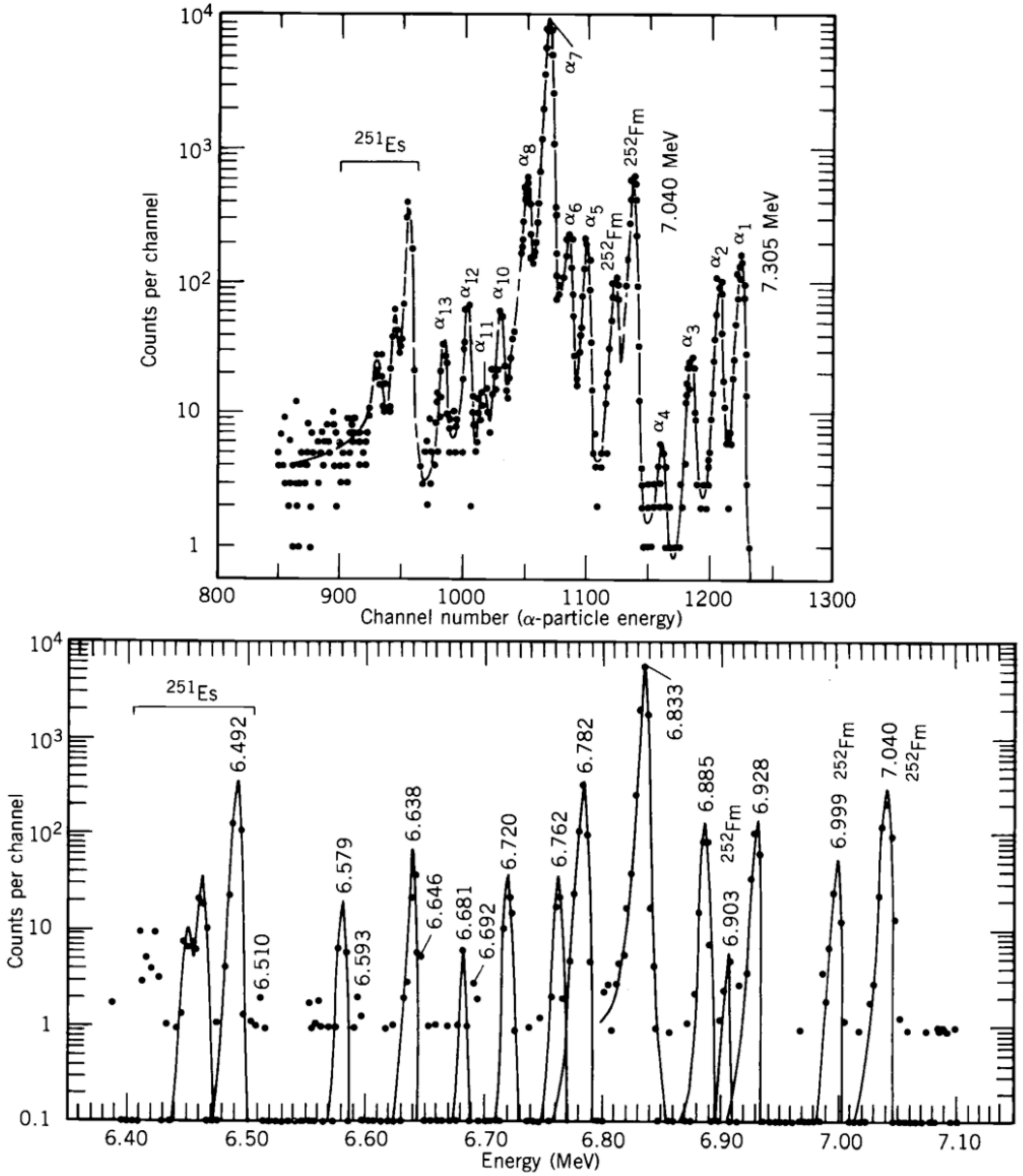

Figure 8.11 α spectrum from the decay of ^{251}Fm. The top portion shows the spectrum as observed with a Si detector. The bottom shows a portion of the same spectrum observed with a magnetic spectrometer, whose superior energy resolution enables observation of the 6.762-MeV decay, which would be missed in the upper spectrum. From Ahmad et al., *Phys. Rev. C* **8**, 737 (1973).

α decay

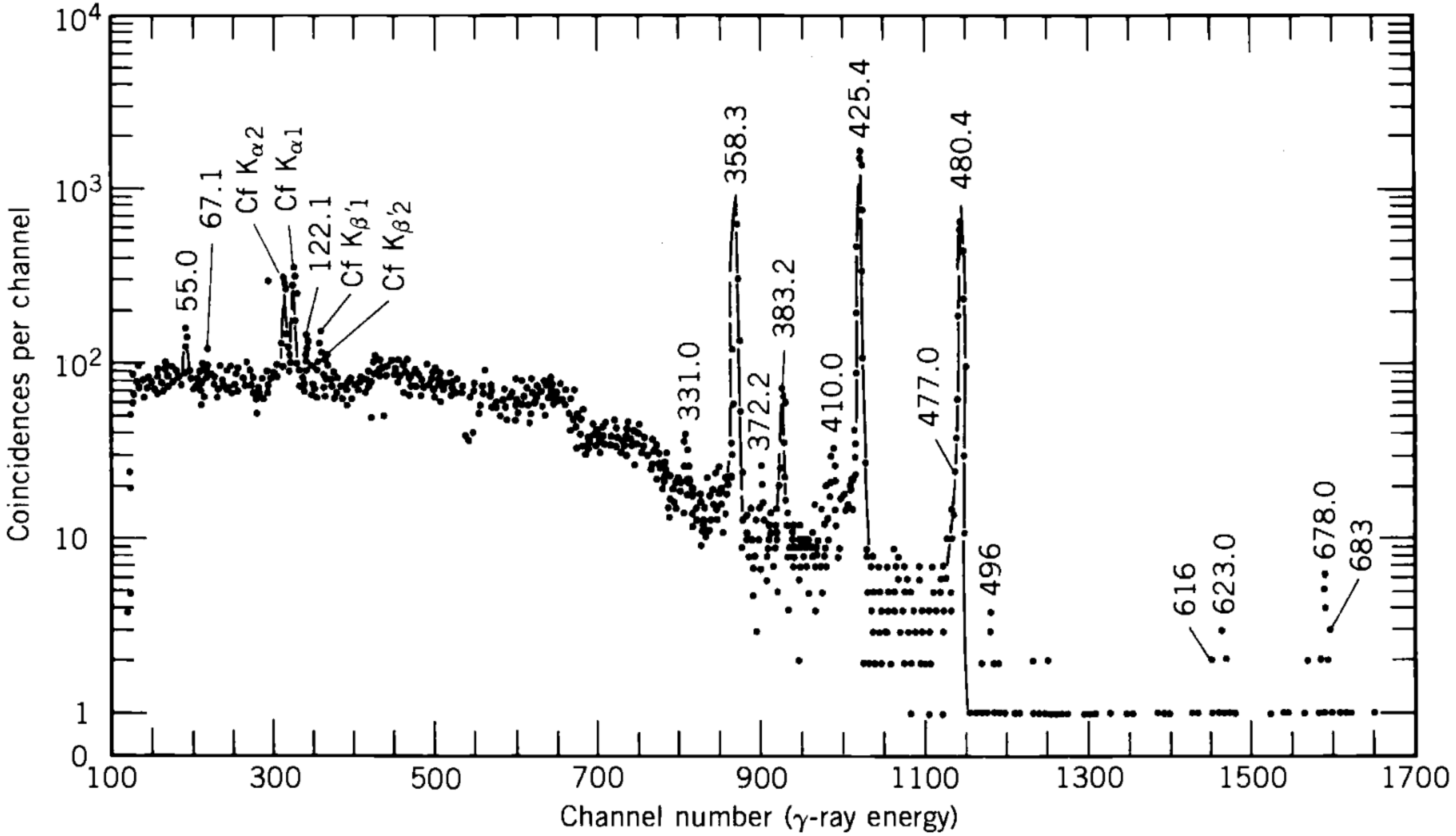

Figure 8.12 γ-ray spectrum of ^{251}Fm in coincidence with all α decays in the range 6.0 to 7.7 MeV. The spectrum was obtained with a Ge(Li) detector.

α decay

Excitation energy levels calculated from the α and γ spectra

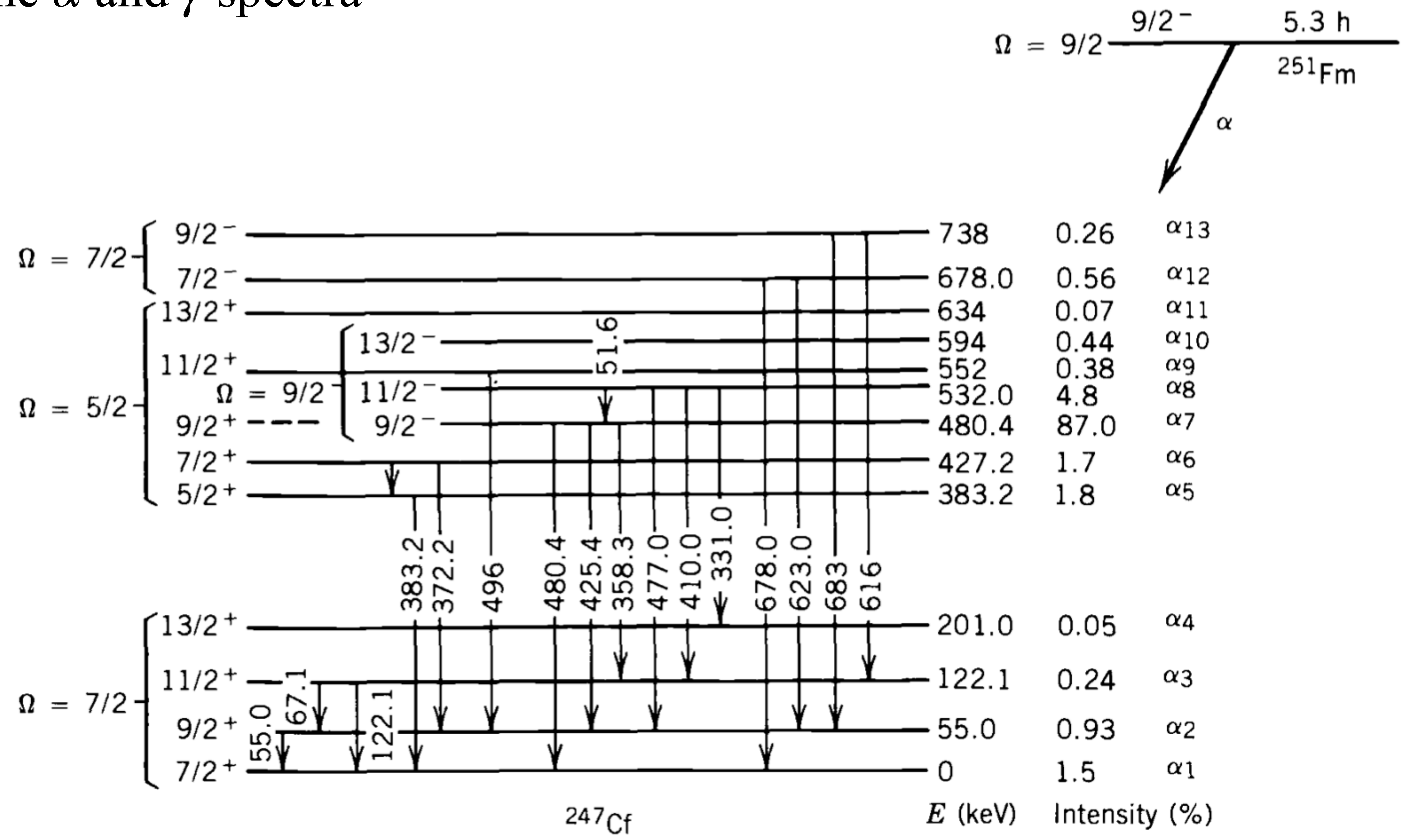

Figure 8.13 The decay scheme of ^{251}Fm to levels of ^{247}Cf deduced from α and γ spectroscopy. The spin assignments for the higher levels are deduced using γ-ray and internal conversion techniques described in Chapter 10.

α decay

1D spectra

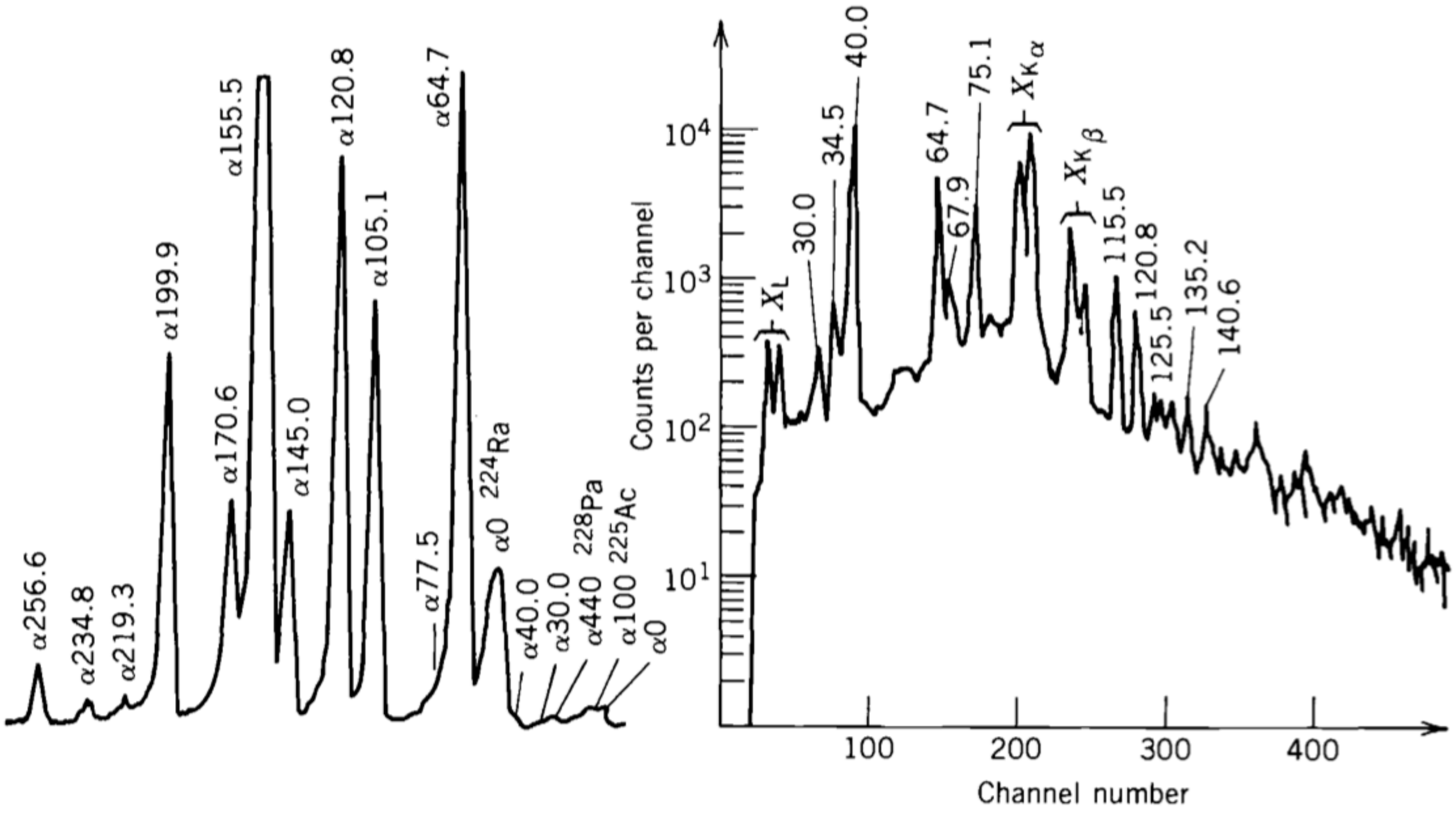

Figure 8.14 α (left) and γ (right) spectra from the decay of ^{229}Pa to ^{225}Ac. The α peaks are labeled according to the excited state populated in ^{225}Ac; thus $\alpha105.1$ indicates the decay leading to the excited state at 105.1 keV. Prominent peaks from impurities are also indicated. The γ spectrum is taken in coincidence with all α's. From P. Aguer et al., *Nucl. Phys. A* **202**, 37 (1973).

α decay

2D spectra

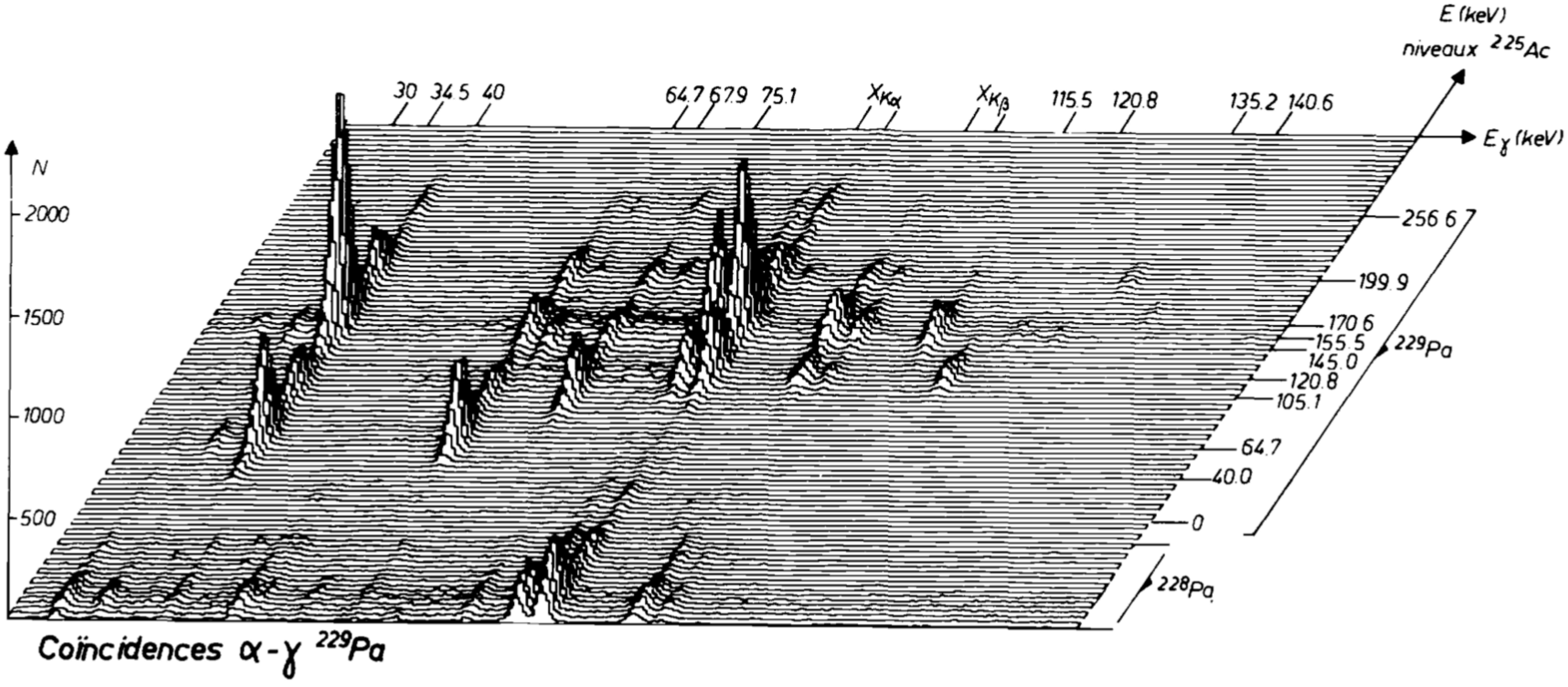

Figure 8.15 Three-dimensional (sometimes called two-parameter) representation of α-γ coincidences in the decay of ^{229}Pa. The horizontal axis shows γ-ray energies, labeled along the top. The oblique axis gives α-decay energies, labeled to indicate the ^{225}Ac state populated in the decay. The vertical axis gives the intensity of the coincidence relationship.

α decay

Energy levels based on the spectra

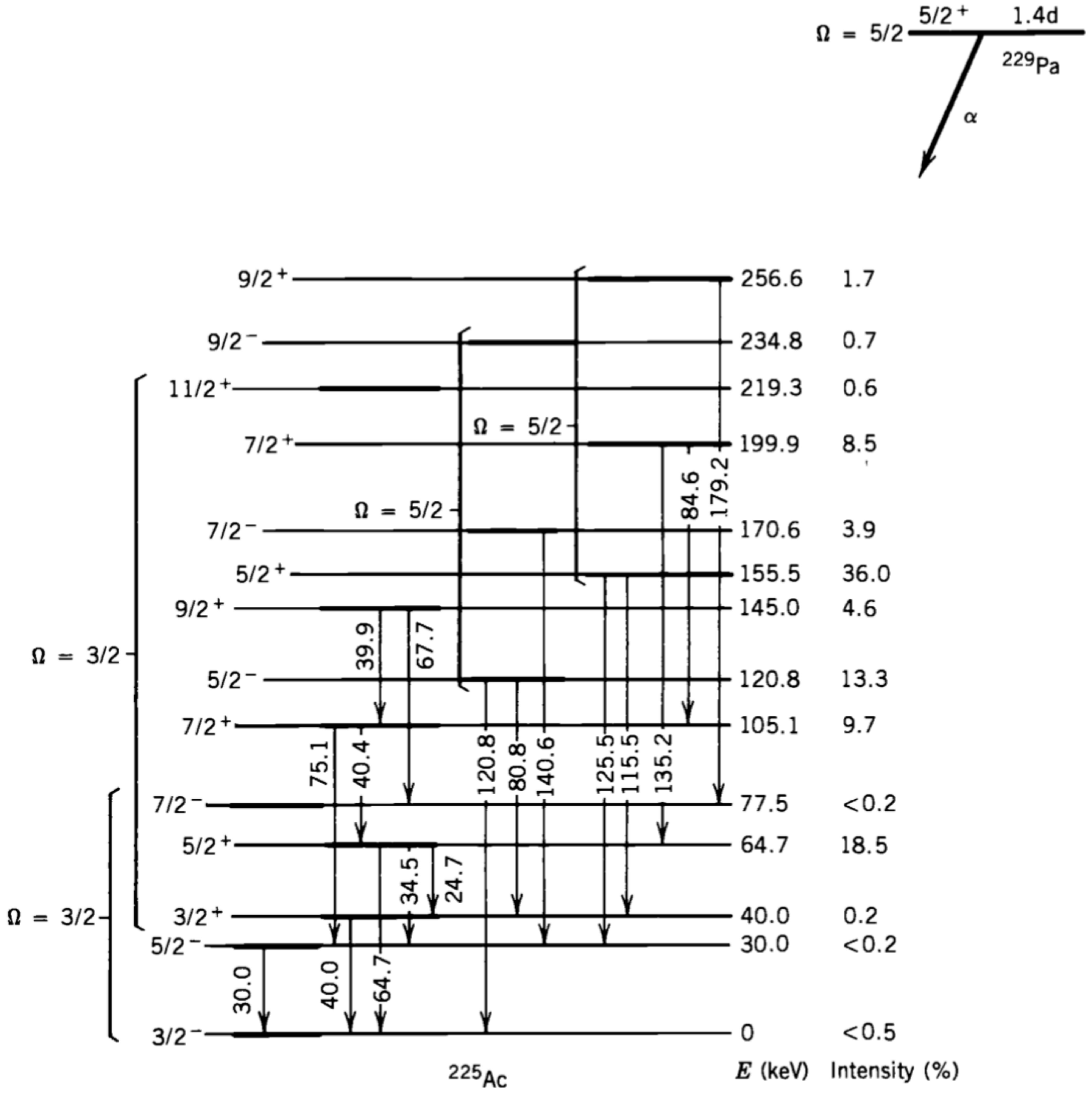

Figure 8.16 Decay scheme of ^{229}Pa deduced from α and γ spectroscopy.